Article

Propylsulfonic Acid Functionalized SBA-15 Mesoporous Silica as Efficient Catalysts for the Acetalization of Glycerol

Ruiyun Li [1,2], Heyuan Song [1,2] and Jing Chen [1,*]

[1] State Key Laboratory for Oxo Synthesis and Selective Oxidation, Lanzhou Institute of Chemical Physics, Chinese Academy of Sciences, Lanzhou 730000, China; liruiyun@licp.cas.cn (R.L.); shy@licp.cas.cn (H.S.)

[2] University of Chinese Academy of Sciences, Beijing 100049, China

* Correspondence: chenj@licp.cas.cn; Tel.: +86-931-4968068; Fax: +86-931-4968129

check for
updates

Abstract: As the main by-product obtained from biomass, glycerol could be converted into valuable chemicals. Tunable propylsulfonic acid functionalized SBA-15 and KIT-6 with different structural parameters have been prepared by different methods while using 3-mercaptopropyltrimethoxysilane (MPTMS) as the source of sulfur. The composition and structure of the synthesized catalysts have been well-characterized by N_2 adsorption-desorption (BET), X-ray diffraction (XRD), X-ray photoelectron spectroscopy (XPS), X-ray fluorescence (XRF), scanning electron microscopy (SEM), and transmission electron microscopy (TEM). The catalytic performance of the prepared catalysts have been evaluated and compared in glycerol acetalization with formaldehyde to the mixture of 1,3-dioxane-5-ol and 1,3-dioxolane-4-methanol. Optimum reaction parameters were investigated to enhance the yield of products and control the distribution of glycerol formals. More than 90% yield of cyclic acetals were obtained with the ratio of two isomers 5R to 6R of 42:58.

1. Introduction

Glycerol (1,2,3-propanetriol or glycerine) is a high value-added by-product of the biodiesel production from the reaction of vegetable oil/triglyceride with alcohols and the amount of glycerol constitutes 10 wt % of total biodiesel production [1,2]. Over 68% of glycerol production was achieved through biodiesel in 2015. In addition, biodiesel is the fastest growing biofuel, which may increase to at least 2700 kilo tons by 2022. The biodiesel market size is expected to witness steady gains over the next seven years, which enable it to account for a significant chunk of glycerol market share [3]. Glycerol is also the production of ethanol fermentation processes [4]. Being a by-product of biodiesel, glycerol supply has ascended rapidly and the already saturated market has been adversely affected [5]. The global glycerol market is segmented as follows by application: polyether polyols, pharmaceuticals, and tobacco humectants, etc., and numerous utilization of glycerol have been studied. To stabilize the glycerol market, the main research was focused on hydrogenolysis [6], etherification [7], hydrogenation [8], partial oxidation [9,10], and dehydration [11]. Acetalization of glycerol with aldehydes/ketones is also one of valorization pathway to balance the glycerol market and acetals/ketals could be widely used in fine organic synthesis [12].

The acetalization production particularly glycerol acetals/ketals have been investigated as fuel additives in gasoline and extensively utilized as protecting group or starting materials in organic synthesis [13], surfactants [14,15], and flavors and pharmaceutical products [16–18]. Acetalization of glycerol with formaldehyde is an important acid catalyzed reaction for the produce of isomeric cyclic

acetals 1,3-dioxolane-4-methanol (five member ring hereafter designated as 5R) and 1,3-dioxane-5-ol (six member ring hereafter designated as 6R) (Scheme 1), which finds applications as a disinfectant and solvent for cosmetics and medical usage [18–20].
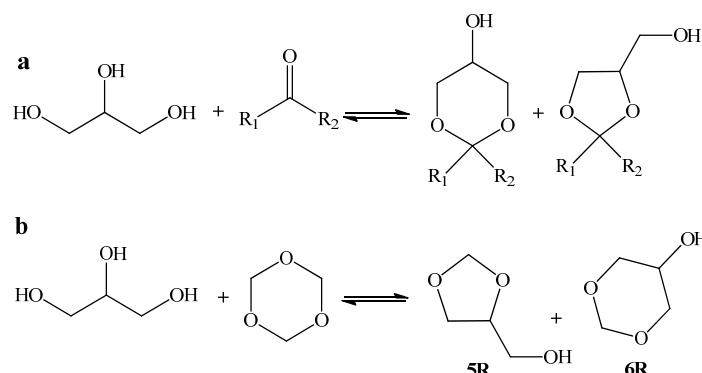
Scheme 1. Glycerol acetalization with aldehydes/ketones.

In terms of catalysts, the acetalization of glycerol is an acid catalyzed reaction and glycerol formals (GF) could be manufactured while using homogeneous catalysts, such as H_2SO_4 [21], HF, HCl, or PTSA [22], giving a 40:60 ratio of 5R to 6R [23]. Acetalization of glycerol with formaldehyde that was performed with PTSA achieved maximum yield (78%) within 2 h and there is no further improvement to prolong reaction times. The preparation of glycerol formal in the presence of different Lewis and Brønsted acid catalysts gave a large spectrum of yield, with 84% being the highest yield reported up to now, with a ratio 5R to 6R of 27:73. However, homogeneous catalysts are toxicant, corrosive, and difficult to separate from the reaction system, which limited the wide application.

In contrast, heterogeneous catalysts have been investigated extensively in recent studies and they present many advantages over homogeneous systems. Acetalization/Ketalization of glycerol using heterogeneous catalysts, like ion exchange resins [24], metal oxides [25,26], and SBA-15 supported $Cs_{2.5}H_{0.5}PW_{12}O_{40}$ [27,28], etc. have been studied. Da Silva et al. [17] investigated the efficiency and the reaction kinetics with solid catalysts, such as Amberlyst-15, H-USY, montmorillonite K-10, and zeolite Beta in comparison with a homogeneous catalyst PTSA in the acetalization of glycerol with acetone and formaldehyde aqueous. Zeolite Bate (Si/Al = 16) leads to a conversion of 95% at 60 min. The conversion of acetone in glycerol acetalization can reach 90% within 40 min. However, the conversion of glycerol acetalization with formaldehyde is only 80%. The yield of glycerol with formaldehyde using Amberlyst-36 can reach 77% and the ratio of 5R to 6R is 24:76 [29].

The ordered mesoporous materials attracted much attention for their high surface areas, controllable pore size, and pore volume. Surface functionalization of molecular sieve is an efficient method to enhance the acid capacity by modifying the surface of mesoporous materials and it has been widely used in the synthesis of Bisphenol-A and biodiesel synthesis [30–32]. Various groups, such as vinyl, thiol (–SH), and amine were successfully used to functionalize the mesoporous materials [33–35]. Acid-functionalized mesoporous silica typically containing propylsulfonic acid has been extensively investigated as an efficient catalyst in acid-catalyzed reaction (esterification, selective acylation, dehydration, hydrolysis, and condensation) [36–38]. SO_3H-functionalized mesoporous silica are commonly generated using 3-mercaptopropyltrimethoxysilane (MPTMS) via oxidation of thiol-propyl groups during the co-condensation or post-grafting oxidation methods. Moreover, sulfonation benefits from higher local hydrophobicity of the sulfonic acid sites [39]. It was acknowledged that mild hydrothermal treatment could be used to activate the surface of molecular sieve and increase its acid capacity for grafting in the sensitive surface. Inorganic salts, such as KCl, NaCl, and NaF, etc. are usually used to moderate the wall thickness and the degree of polymerization during post-synthesis hydrothermal treatments of SBA-15 [40], and also aid in the dissolution of silica. Thus, we hypothesized

that the addition of NaCl under mild hydrothermal conditions could promote the activation of SBA-15 surfaces for grafting [41].

In this paper, an array of propylsulfonic acid functionalized mesoporous silicas SBA-15 and KIT-6 were prepared and catalytic performance of synthesized catalysts in glycerol acetalization with formaldehyde were investigated. We also used NaCl as additive in the process of catalyst preparation [42]. The synthesized catalysts were characterized by N_2 adsorption-desorption (BET), X-ray diffraction (XRD), scanning electron microscopy (SEM), transmission electron microscopy (TEM), X-ray fluorescence (XRF, bulk), X-ray photoelectron spectroscopy (XPS, surface), and acid capacity based on acid-base titration. Moreover, the effect of various reaction parameters, such as reaction time, reaction temperature, molar ratio of formaldehyde to glycerol, and catalyst loading were studied to enhance the yield of isomeric products. The distribution of the 5R and 6R was also investigated.

2. Results and Discussion

2.1. Materials Characterization

In this section, $PrSO_3H$-SBA-15-x (x = 0, 200, 400, 800) is the propylsulfonic acid functionalized SBA-15 mesoporous silica synthesized by post-grafting with different amount of additive. $PrSO_3H$-SBA-15-OP was materials synthesized by one-pot method and $PrSO_3H$-SBA-15-Tol means materials that was synthesized by the co-condensation method. $PrSO_3H$-KIT-6-T were catalyst synthesized by co-condensation method and aged at different temperature (80 °C, 100 °C, or 120 °C).

The successful synthesis of parent and grafting ordered mesoporous silica SBA-15 and KIT-6 were first assessed by XRD and BET. The structure and composition of the samples were identified by XRD and XPS. Powder XRD patterns of small-angle range of the series of $PrSO_3H$-SBA-15 synthesized by different methods are presented in Figure 1. All of the functionalized materials show similar XRD patterns with common reflections at 0.8°, which is consistent with the parent SBA-15 and confirms that grafting of propylsulfonic acid group (–$PrSO_3H$) and subsequent oxidation does not alter the crystal structure. The structural integrity of precursor is retained after both functionalization by –$PrSO_3H$ in H_2O using NaCl as additive and oxidation by H_2O_2.
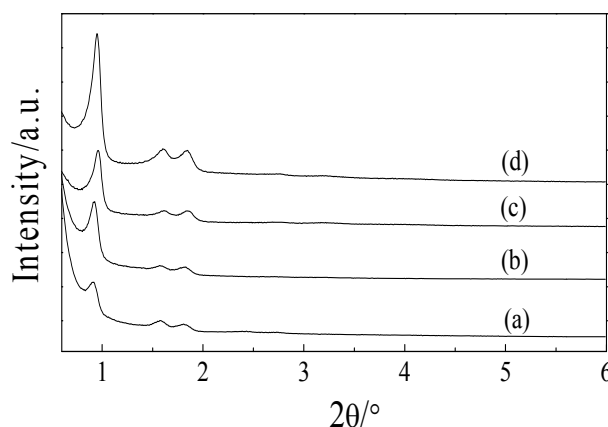
Figure 1. Small-angle X-ray diffraction (XRD) patterns of mesoporous silica: (a) SBA-15; (b) $PrSO_3H$-SBA-15-400; (c) $PrSO_3H$-SBA-15-Tol; and, (d) $PrSO_3H$-SBA-15-OP.

Figure 2 compares the corresponding N2 adsorption–desorption isotherms and pore size distributions curves of the precursor and sulfonated mesoporous materials, which best represents the characteristics of all the samples. It could be observed that most of the samples isotherms are of Type IV with H1 hysteresis loops, which is the characteristic of mesoporous materials. However, $PrSO_3H$-SBA-15-OP and KIT-6-80 are of Type IV with mixed H1-H2-type hysteresis loops. The presence of parallel adsorption and desorption branches suggests the existence of mesoporous

structure. Different hysteresis loop occurred at two-dimensional (2D) hexagonal (SBA-15) and three-dimensional (3D) cubic (KIT-6) structures. The calculation from the desorption branch using the Barrett-Joyner-Halenda (BJH) method (Figure 2A) shows that the catalysts present a very narrow pore size distribution. The physical-chemical parameters of various samples are summarized in Table 1. Surface areas were calculated on the basis of Brunauer-Emmett-Teller (BET) equation and pore sizes by the Barrett-Joyner-Halenda (BJH) method. There is an obvious decrease in BET surface area, pore diameter, and pore volume when -$PrSO_3H$ is grafted on the mesoporous materials. The pore diameter of sulfonated SBA-15 synthesized by post-grafting using NaCl as additive is higher than that of conventional method by one-pot method. The surface area of catalysts synthesized by post-grafting method with different amount of NaCl range from 281.19 m^2/g to 410.46 m^2/g and pore volumes range from 0.54 cm^3/g to 0.87 cm^3/g. Pore system of molecular sieve SBA-15 consists of hexagonally ordered mesoporous and irregular microporous [43]. The decrease of the surface area may be caused by the blockage of the micropore during the grafting. $PrSO_3H$-SBA-15 exhibits the smallest surface area and highest bulk sulfur and acid content, which indicates the maximal grafting loading of propylsulfonic acid groups. The broad distribution curves of SBA-15 when compared to that of SBA-15 in previous report may be due to the quality of commercial SBA-15.

Table 1. Properties of propylsulfonic acid functionalized SBA-15 and KIT-6.

Samples	Surface Area [a]/ m^2g^{-1}	Pore Volume/cm^3g^{-1}	Average Pore Diameter [b]/ nm	Bulk S Content [c]/ wt %	Surface S Content [d]/ wt %	Acid Capacity [e]/ mmol g^{-1}
SBA-15	541	1.30	9.8	−	−	−
$PrSO_3H$-SBA-15-Tol	464	1.08	9.9	0.14	3.36	0.43
$PrSO_3H$-SBA-15-OP	674	0.52	3.1	0.06	1.38	0.22
$PrSO_3H$-SBA-15-0	410	0.87	8.5	4.87	5.30	1.03
$PrSO_3H$-SBA-15-200	325	0.54	6.7	6.22	3.60	1.11
$PrSO_3H$-SBA-15-400	281	0.58	8.2	8.50	3.74	1.17
$PrSO_3H$-SBA-15-800	296	0.66	8.9	8.07	3.42	1.09
KIT-6-80	539	0.57	4.3	−	−	−
$PrSO_3H$-KIT-6-80	362	0.37	4.1	1.34	2.56	0.67
$PrSO_3H$-KIT-6-100	443	0.42	3.8	5.90	5.21	0.60
$PrSO_3H$-KIT-6-120	402	0.44	4.4	2.03	4.95	0.55

[a] BET, [b] BJH, [c] XRF, [d] XPS, [e] total acidity determined by base-acid titration.


(A)
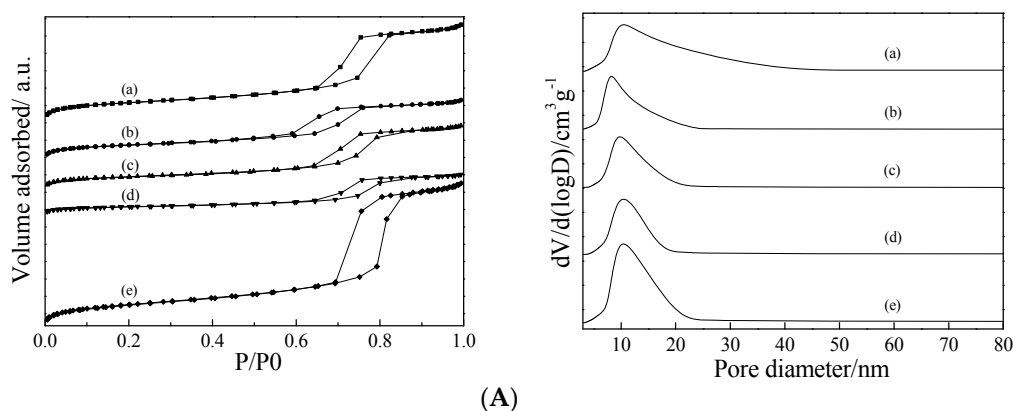
Figure 2. *Cont.*
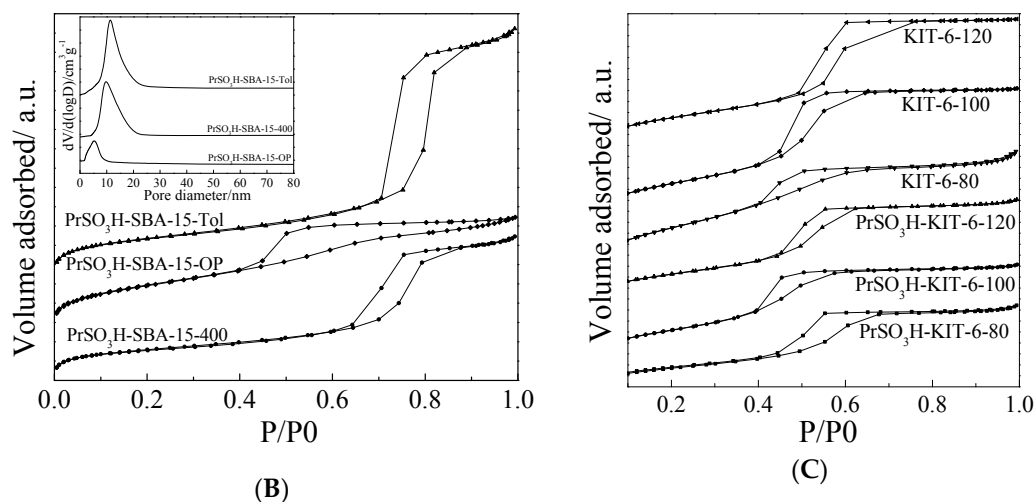
Figure 2. (**A**) N$_2$ adsorption–desorption isotherms and pore size distributions curves of (a) PrSO$_3$H-SBA-15-0; (b) PrSO$_3$H-SBA-15-200; (c) PrSO$_3$H-SBA-15-400; (d) PrSO$_3$H-SBA-15-800; (e) SBA-15. (**B**) N$_2$ adsorption–desorption isotherms and pore size distributions curves of PrSO$_3$H-SBA-15-400; PrSO$_3$H-SBA-15-OP; and PrSO$_3$H-SBA-15-Tol. (**C**) N$_2$ adsorption–desorption isotherms and pore size distributions curves of KIT-6 family.

Complete grafting of thiol-propyl groups on mesoporous materials and the following oxidation to sulfonic acid groups were examined by XRF and XPS. As could be deserved by the bulk sulfur content of the catalysts that were determined by XRF in Table 1, the bulk sulfur content of PrSO$_3$H-SBA-15 synthesized by one pot method and conventional method is 0.06 wt % and 0.14 wt %, respectively. Higher grafting amount of propylsulfonic acid groups was achieved by post-grafting in H$_2$O using NaCl as additive. The relation between bulk sulfur content and acid site also suggests the complete oxidation of thiol-propyl groups, which is consistent with the results of XPS. As shown in S2p XP spectra of both sulfonic acid functionalized materials (Figure 3), a single energy doublet that was caused by propylsulfonic acid groups centered at 168.9 eV, which revealed that a single S chemical environment appeared, confirming the complete oxidization of thiol-propyl groups to propylsulfonic acid groups [44–46]. It is also notable that surface sulfur amounts range from 3.60 wt % to 5.23 wt % with the amount of NaCl changing from 0 to 800 mg. PrSO$_3$H-SBA-15-400 has the highest bulk S content and smaller pore volume. The concentration of active Si–OH on molecular sieve SBA-15 have an important influence on the grafting efficiency [47]. A higher propylsulfonic acid amount is obtained on SBA-15 than the family of KIT-6 by comparing of the bulk and surface sulfur, which suggests the higher density of reactive silicone groups on SBA-15.
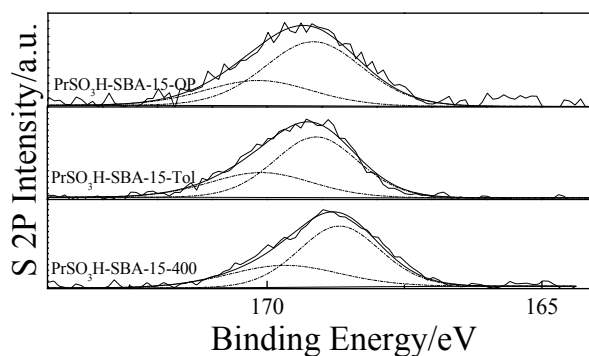

Figure 3. *Cont.*
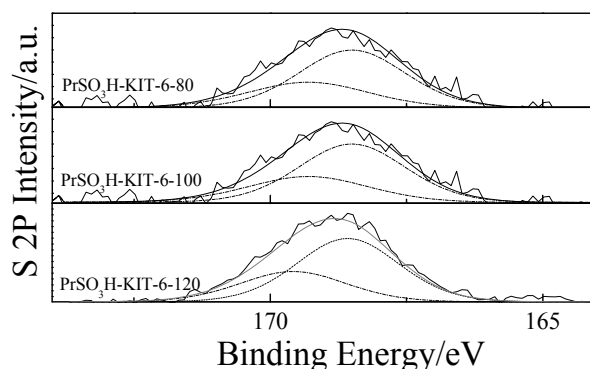
Figure 3. Fitted S2p spectra for PrSO$_3$H-SBA-15 and PrSO$_3$H-KIT-6 materials.

The synthesis of propylsulfonic acid functionalized mesoporous silica includes the grafting of –SH and successful oxidation of –SH to –SO$_3$H by hydrogen peroxide (H$_2$O$_2$) [48]. Oxidation of the –SH to –SO$_3$H is necessary to enhance the acid strength of molecular sieve and to obtain catalysts with good catalytic activity. The ideal oxidation of –SH to –SO$_3$H should be proceeded with the following reaction (R–SH + 2H$_2$O$_2$→R–OSO$_2$H + 3H$_2$O). The acidic properties of the grafted sulfonic acid catalysts were measured by acid-base titration. As shown in Table 1, the acid capacity for NaCl added PrSO$_3$H-SBA-15 was found to be two to three times higher than PrSO$_3$H-SBA-15-Tol.

By SEM and TEM, the shape of the primary crystallites and the order of their packing in catalysts were examined. From SEM images (Figure 4b), we can see that these materials are consisted of some short rods with a relatively uniform length and the short-rod morphology of SBA-15 sample was well preserved after grafting (Figure 4b,c). The TEM image of SBA-15 (Figure 5a) shows well-ordered hexagonal arrays of mesopores and confirms its 2D hexagonal structure. The TEM observations also indicated that ordered mesostructured of SBA-15 and KIT-6 were retained, even after post-grafting. As an exception, the image of PrSO$_3$H-SBA-15-OP is different from the others, which is consistent with the N$_2$ isotherms in Figure 2B.
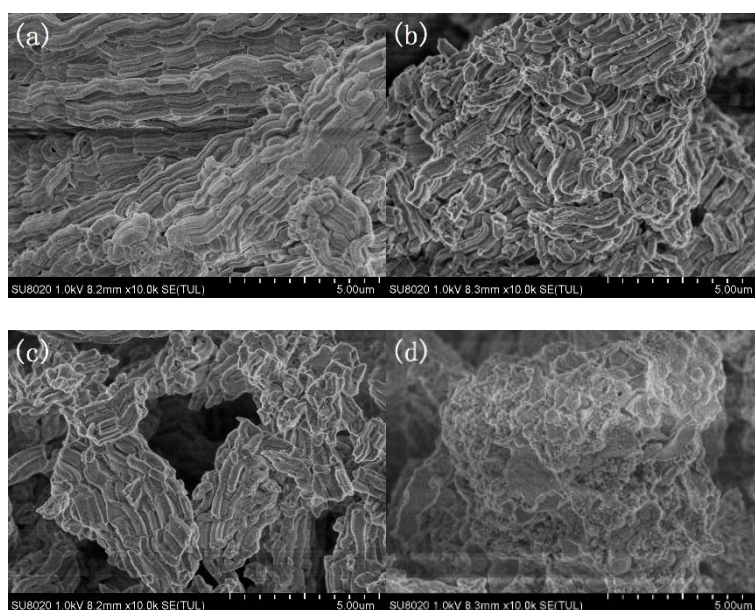
Figure 4. Scanning electron microscopy (SEM) images of (**a**) SBA-15; (**b**) PrSO$_3$H-SBA-15-400; (**c**) PrSO$_3$H-SBA-15-Tol; and, (**d**) PrSO$_3$H-SBA-15-OP.
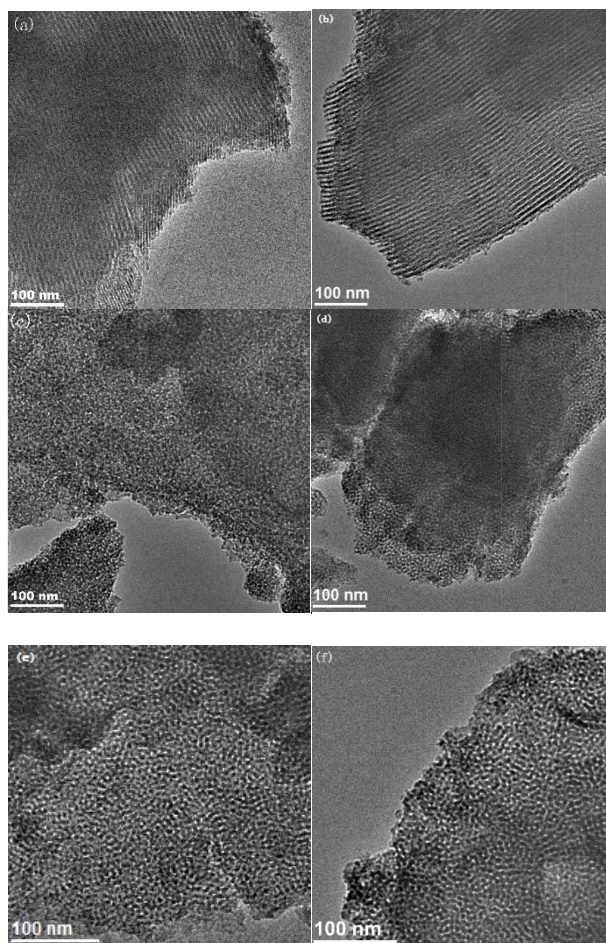
Figure 5. Transmission electron microscopy (TEM) images of parent and propysulfonic acid functionlized SBA-15 and KIT-6: (**a**) SBA-15; (**b**) PrSO$_3$H-SBA-15-400; (**c**) PrSO$_3$H-SBA-15-Tol; (**d**) PrSO$_3$H-SBA-15-OP; (**e**) KIT-6-80; and, (**f**) PrSO$_3$H-KIT-6-80.

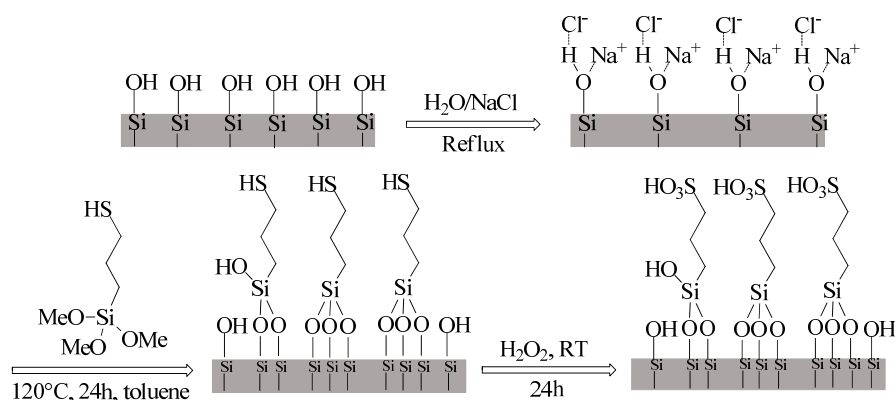## 2.2. Catalytic Activity for Glycerol Acetalization

Propylsulfonic acid functionalized mesoporous materials were prepared by different methods and evaluated in the glycerol acetalization with TOX to obtain the mixture of the glycerol formal (Scheme 1, 5R and 6R). It is clear that all sulfonated mesoporous molecular sieves exhibit higher activity than the non-sulfonated parent material. The gap between the performance of sulfonated and non-sulfonated one is owed to the higher accessibility of reactants to the acidic sites of sulfonated catalysts.

Figure 6 shows the yield of glycerol formal and the ratio of 5R to 6R achieved by three different source of formaldehyde (FA): 1,3,5-trioxane (TOX), formaldehyde solution (FA), and paraformaldehyde (PF). When compared with the results that were obtained with the three source of formaldehyde, TOX shows the best yield of glycerol formal and the ratio of 5R to 6R is 42:58. Herein, we used TOX as the source of FA for the further study.
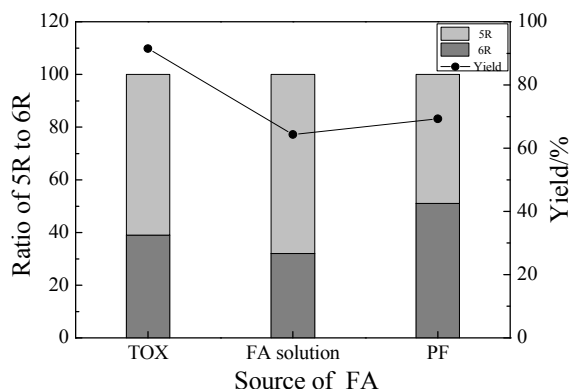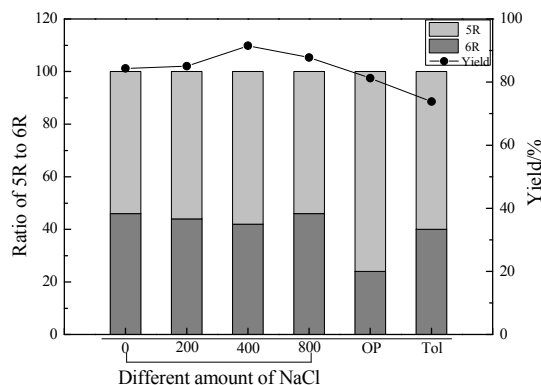
Figure 6. Effect of different source of formaldehyde on the glycerol acetalization catalyzed by PrSO₃H-SBA-15-400. Reaction condition: glycerol (4.60 g, 50 mmol), TOX (2.25 g, 75 mmol), 0.2 g catalysts, bath temperature 90 °C, reaction time 8 h.

Inorganic salt NaCl is used to control the pore parameters (pore size, wall thickness, and surface area, etc.) and the degree of polymerization during post-grafting. The possible role of NaCl in promoting grafting amount is presented in Scheme 2. Ionic interactions with Cl⁻ to open the Si–O–Si bridges and activate Si–OH of the molecular sieve in a mixture of H_2O and NaCl.

Scheme 2. Possible role of NaCl in activating siloxane bridges for grafting.

The effect of the amount of NaCl during sulfonation and the catalytic activity of the synthesized catalysts on glycerol acetalization were studied. Figure 7 showed the catalytic properties of the series of PrSO₃H-SBA-15-x (x = 0, 200, 400, 800). Post-grafting synthesized SBA-15 catalysts apparently exhibited higher catalytic performance than the one-pot method and conventional toluene grafted method in the described reaction. When the amount of NaCl is 400 mg, the catalyst has the smallest surface area and highest acid capacity. PrSO₃H-SBA-15-400 presented the greatest catalytic performance. The yield of 5R + 6R can reach 91.5% and the ratio of 5R:6R is 42:58. The catalytic activity of the prepared catalysts using different methods increased in the order: PrSO₃H-SBA-15-400 > PrSO₃H-SBA-15-OP > PrSO₃H-SBA-15-Tol. According to acid-base titration, the acid capacity of the series of PrSO₃H-SBA-15 range from 0.2 mmol g^{-1} to 1.2 mmol g^{-1}, which is in agreement with the catalytic performance. That is to say, the catalysts that were synthesized by post-synthesis method exhibited higher catalytic performance than the conventional methods.

Figure 7. Catalytic performance of PrSO$_3$H-SBA-15 with different methods in glycerol acetalization. Reaction condition: glycerol (4.60 g, 50 mmol), TOX (2.25 g, 75 mmol), 0.2 g catalysts, bath temperature 90 °C, reaction time 8 h.

In previous work, the investigations were aiming at increasing the amount of 1,3-dioxan-5-ols (6R) because 6R could be used as raw materials of 1,3-propanediol derivatives. The product distribution of glycerol acetalization with TOX (Scheme 1, 5R and 6R) is highly dependent on the experimental conditions. Therefore, PrSO$_3$H-SBA-15-400 was used to optimize the reaction condition to reach a high yield of the isomers and ratio of 6R.

Effect of catalyst content: To optimize the amount of catalyst for glycerol acetalization with TOX, the reaction was conducted over PrSO$_3$H-SBA-15-400 for 8 h at 90 °C using a different amount of catalyst (Figure 8). The yield of glycerol formal was increased from 85.7% to 91.5% by increasing the catalyst amount from 2 wt % to 4 wt %. However, there is no further enhance was achieved and the ratio of 6R decreased gradually when increasing the catalyst amount to 6 wt %.
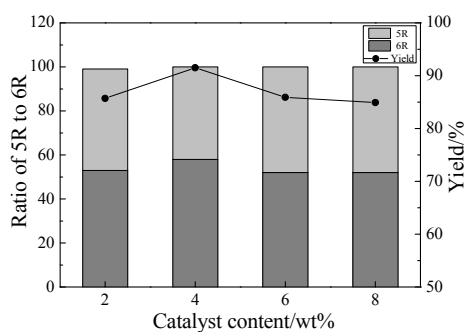
Figure 8. Effect of catalysts content on the yield of glycerol formals (GF) over PrSO$_3$H-SBA-15-400 with reactant molar ratio (formaldehyde: glycerol) 1.5:1 at 90 °C for 8 h.

Effect of reaction temperature: Figure 9 showed the effect of temperature variation on the acetalization of glycerol with formaldehyde. Several tests were conducted at different temperature from 40 °C to 120 °C to acquire the optimal parameter. The yield of GF changed from 18.5% at 60 °C to 91.5% at 90 °C. The amount of 6R increased at first with the temperature ranging from 40 °C to 90 °C. However, 6R isomer decreased quickly after 90 °C, which may be caused by the isomerization of the 5R to 6R.
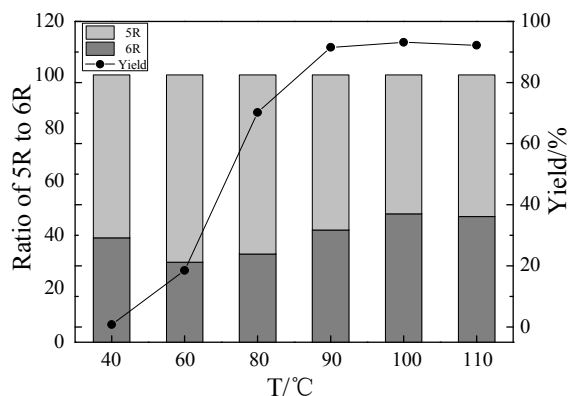
Figure 9. Effect of temperature on the yield of GF over PrSO$_3$H-SBA-15-400 using 0.2 g catalysts, reactant molar ratio (formaldehyde: glycerol) 1.5:1 for 8 h.

Effect of mole ratio of formaldehyde to glycerol: The catalytic experiments were carried at 90 °C, 8 h with a catalyst amount of 4 wt %, formaldehyde/glycerol = 1:1, 1.5:1, 2:1, 3:1. Figure 10 indicates the yield of GF and the distribution of the glycerol formal that is influenced by the change of molar ratio of formaldehyde to glycerol. The yield of GF increases from 83.7% to 91.5% when the mole ratio of formaldehyde to glycerol increasing from 1.2:1 to 1.5:1. Further increasing molar ratio from 1.5:1 to 3:1, the yield of GF decreased to 61.0% and the ratio of 6R decreased slightly.
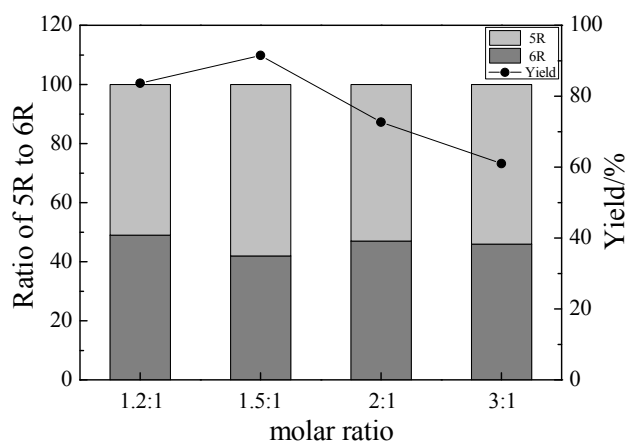
Figure 10. Effect of mole ratio (formaldehyde to glycerol) on the yield of glycerol formal over 0.2 g PrSO$_3$H-SBA-15-400 at 90 °C for 8 h.

Effect of reaction time: The experiments were carried out from 1 h to 16 h over PrSO$_3$H-SBA-15-400 while using 0.2 g catalysts at 90 °C (Figure 11). The yield increased rapidly by increasing the reaction time to 8 h and reached 91.3%. There is no further increase in the GF yield while extending the reaction time and 6R is decreased gradually.
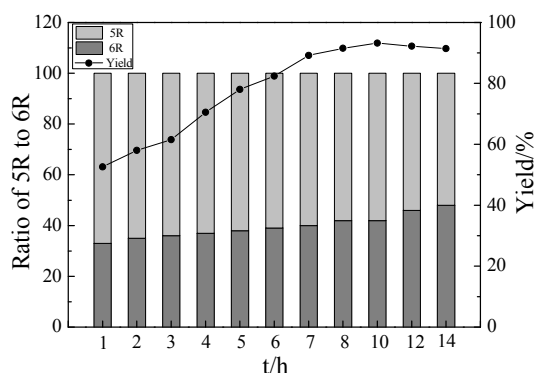
Figure 11. Effect of reaction time on the yield of GF over 0.2 g PrSO$_3$H-SBA-15-400 catalyst at 90 °C with reactant molar ratio (formaldehyde: glycerol) 1.5:1.

Hence, the glycerol acetalization was conducted in solvent free condition while using TOX as the source of formaldehyde. The optimum condition is: 4 wt % catalysts amount, formaldehyde: glycerol 1.5:1 at 90 °C for 8 h, and optimal catalyst activity is 91.5% yield of GF and the ratio of 5R to 6R is 42:58.

We then investigated KIT-6 catalyst family in glycerol acetalization under the optimal reaction parameters and compared the PrSO$_3$H-SBA-15 family with PrSO$_3$H-KIT-6. PrSO$_3$H-KIT-6 was synthesized under different aging temperature for 24 h and the aging temperature showed a dramatic effect on the physical properties and the grafting amount of –SO$_3$H. Different aging temperature expands the surface area from 362 m^{2}g^{-1} to 443 m^{2}g^{-1} and it leads to the decrease of wall thickness, which is in accordance with the literature.

As summarized in Table 2, PrSO$_3$H-KIT-6-80 showed optimal performance for the acetalization of glycerol with formaldehyde (Table 2, Entry 2). The yield of 5R + 6R can reach 89.6%, and the ratio of 5R:6R is 34:66. The SBA-15 supported propylsulfonic acid functionalized catalysts showed a slightly higher yield of GF than KIT-6 supported catalysts (Table 2, Entries 2, 5). However, the ratio of isomer 6R catalyzed by the series of KIT-6 is obviously higher than the series of SBA-15. SBA-15 possesses parallel mesopore channels organized in hexagonal arrangement which may provide better transportation channels to get more access to acid sites. As shown in Table 1, the pore volume and pore size of the series of KIT-6 is smaller than propylsulfonic acid functionalized SBA-15. Maybe much microporosity in KIT-6 hinder the diffusion of bulky molecules, resulting in a low activity of the catalysts.

**Table 2.** Glycerol acetalization with 1, 3, 5-trioxane (TOX) using KIT-6 family catalysts.

Entry	Cat	Yield of GF/%	Ratio of 5R to 6R
1	KIT-6-80	6.0	22:78
2	PrSO$_3$H-KIT-6-80	89.6	34:66
3	PrSO$_3$H-KIT-6-100	85.6	38:62
4	PrSO$_3$H-KIT-6-120	66.6	37:63
5	PrSO$_3$H-SBA-15-400	91.5	42:58

Reaction condition: glycerol (4.60 g, 50 mmol), TOX (2.25 g, 75 mmol), 0.2 g catalysts, bath temperature 90 °C, reaction time 8 h.

2.3. Reaction Mechanism

The formation of GF isomers depend on which two –OH groups joined because of one glycerol molecule has two different hydroxyl groups (–OH). According to da Sliva Ferreira and Sharma S.P. [49,50], the reaction mechanism for the acetalization of glycerol with formaldehyde mainly contains two reversible steps. As shown in Scheme 3, firstly, formaldehyde reacts with the two different –OH groups of glycerol to form two kinds of hemiacetals: 1,2-propanediol, 3-(hydroxymethoxy), and 1,3-propanediol, 2-(hydroxymethoxy). Then, two hydroxyl groups of the hemiacetal condense

and form the two glycerol formal isomers 5R and 6R. From the hemiacetal, 1,2-propanediol, 3-(hydroxymethoxy), two kinds of acetal 5R and 6R can be formed, while for 1,3-propanediol, 2-(hydroxymethoxy), only the 5R acetal is formed. Therefore, the fraction of 5R isomer is always higher than 6R. The first step of converting glycerol to hemiacetal is a fast reaction, while the second step that transforms hemiacetal to the product glycerol formal isomers is slow. However, the hemiacetal cannot be detected by GC, owing to the high injector temperature requested for analysis [51].
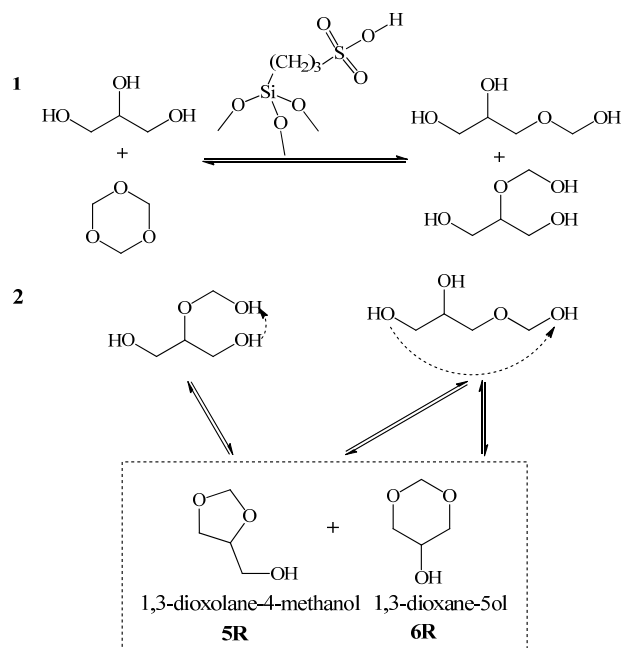
Scheme 3. Possible reaction mechanism for glycerol acetalization with TOX.

2.4. Catalyst Reusability

Finally, we evaluated the recyclability of the PrSO$_3$H-SBA-15-400 in the yield of glycerol acetalization and the distribution of isomers under the optimized conditions (Figure 12). In each cycle, the catalyst was easily separated and recovered from the reaction mixture, washed with dichloromethane, and subsequently dried in vacuum before another reaction was performed. The yield of glycerol formal can reach 79.4% in the fifth runs.
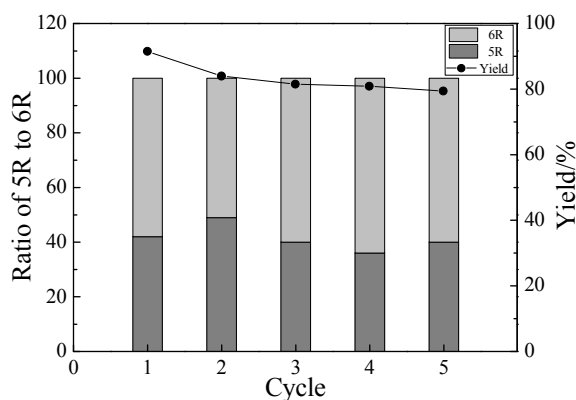
Figure 12. Recyclability of PrSO$_3$H-SBA-15-400 in glycerol acetalization. Reaction condition: glycerol (4.60 g, 50 mmol), TOX (2.25 g, 75 mmol), 0.2 g catalysts, bath temperature 90 °C, reaction time 8 h.

3. Experimental

3.1. Chemicals and Materials

Molecular sieve SBA-15 was purchased from Nanjing XFNANO Materials Tech Co., Ltd. (Nanjing, China). Triblock copolymer $EO_{20}PO_{70}EO_{20}$ (Pluronic P123, MW = 5800) and 3-mercaptopropyltrimethoxysilane (MPTMS, 95%) were purchased from Aldrich Chemical Inc. (Shanghai, China). Toluene, hydrogen peroxide, anhydrous ethanol, and methanol were purchased from Rianlon Chemical Co., Ltd. (Tianjin, China). All of the chemicals are of analytical reagents (A.R.) and used directly without further purification.

3.2. Catalysts Preparation

Sulfonated mesoporous materials were prepared with different methods by varying the synthetic strategies. Molecular sieve KIT-6 were synthesized by the methods of Ryoo et al. [52]. 4 g of Pluronic P123 and 7.5 g of 35% HCl were dispered in 144 g distilled water. The solution was stirred for 2 h at 35 °C and 4 g butanol was added. After stirring for 1 h, 8.5 g of TEOS was added at 35 °C (P123:HCl:TEOS:H_2O:BuOH = 0.017:1.83:1:195:1.31 in mole ratio). The mixture was then agitated for 24 h at 35 °C, and aged for a further 24 h at 80 °C, 100 °C, or 120 °C in a closed polypropylene bottle under static conditions. The solid product obtained was then filtered and dried at 70 °C in vacuum followed by calcination at 550 °C for 5 h.

$PrSO_3H$-SBA-15-OP was synthesized by one pot method as the known procedure that was described by Stucky and his co-workers [53–55]. In a typical preparation procedure, 4 g of Pluronic 123 was dissolved in 125 mL of 1.9 M HCl solution at 40 °C and 8.2 mL of TEOS was added subsequently. After 45 min pre-hydrolysis of TEOS, 0.76 mL of MPTMS and 3.8 mL of H_2O_2 was added. The resultant solution was stirred for 24 h at room temperature, after which the mixture was aged at 100 °C for 24 h under static conditions. The solid was filtered, washed three times with water, and finally dried overnight. The catalyst was labeled as $PrSO_3H$-SBA-15-OP. $PrSO_3H$-SBA-15-Tol was prepared by a co-condensation method [56]. 1 g SBA-15 was dispersed in 30 mL toluene and 1 mL 3-mercaptopropyltrimethoxysilane (MPTMS) was added. The mixture was then refluxed at 130 °C with stirring for 24 h, and the resulting thiol-functionalized product was filtered, washed three times with methanol, and dried on vacuum at RT. –SH was converted into –SO_3H by mild oxidation with 30 mL of 30% hydrogen peroxide by continuous stirring at room temperature for 24 h. The sulfonated solid product was subsequently filtered, washed three times with methanol, and dried in vacuum. The product was labeled as $PrSO_3H$-SBA-15-Tol.

The series of $PrSO_3H$-SBA-15-x was prepared by the following method: 1 g SBA-15 and x mg NaCl were added to 30 mL H_2O and stirred for 15 min. Subsequently, 1 mL MPTMS was added to the solution and refluxed under stirring at 100 °C for 24 h, after which the resulting thiol-propyl modified solids catalysts were filtered, washed three times with H_2O, and dried in vacuum. Oxidation of –SH to the –SO_3H was conducted in 30 mL of 30% hydrogen peroxide at RT for 24 h. The propylsulfonated solid products were filtered, washed three times with methanol, and dried in vacuum. The resulting sulfonic acid derivatized catalysts were denoted as $PrSO_3H$-SBA-15-x (where x represents the amount of NaCl mg used in the grafting process).

The series of $PrSO_3H$-KIT-6-T was synthesized by the following method: 1 g of KIT-6 synthesized under different aging temperature and 1 mL of MPTMS were added to 30 mL toluene. The mixture was then refluxed with stirring at 130 °C for 24 h and the resulting thiol-functionalized solid product was filtered, washed three times with methanol, and dried at 70 °C in vacuum. The conversion of thiol-propyl groups to –SO_3H was consistent with the procedure described above. The synthesized catalyst was marked as $PrSO_3H$-KIT-6-T.

3.3. Catalyst Characterization

Structural properties and composition of prepared mesoporous materials were measured by a combination of N_2 adsorption-desorption (BET), and X-ray diffraction (XRD), scanning electron microscopy (SEM), transmission electron microscopy (TEM), with sulfur content determined by X-Ray (XRF, bulk) and X-ray photoelectron spectroscopy (XPS, surface), and acid capacity based on acid-base titration.

N_2 adsorption-desorption isotherms were recorded while using a TristarII 3020 instrument (Norcross, GA, USA) and pore size distribution curves were calculated from the analysis of desorption branch of the isotherm by the BJH (Barrett-Joyner-Halenda) method. Surface areas were calculated using the Brumauer-Emmett-Teller (BET) method over the relative pressure range at $P/P_0 = 0.06–0.28$. Before adsorption, the samples were degassed at 423 K for 4 h.

Powder X-ray diffraction (XRD) patterns were collected on a PANalytical Empyrean (Almelo, Netherlands). Small-angle X-ray diffraction patterns were acquired from $2\theta = 0.3°$ to $6°$ with a $0.01°$ step size.

Transmission electron microscopy (TEM) images were recorded on a FEI microscope (Hillsboro, OR, USA) operated at 200 kV equipped with a Gatan K2 Summit camera. Sample were prepared by dispersing in ethanol and dropcasting onto a micro grid. Scanning electron microscopy (SEM) photos were taken with a Model SU8020 (Hitachi, Japan) field emission scanning electron microscopes.

X Ray Fluorescence (XRF) was performed on a PANalytical Magix PW2403 (Almelo, Netherlands). XPS was performed using an ESCALAB 250Xi instrument (Loughborough, UK) fitted with a charge neutralizer and neutraliser and magnetic focusing lens employing Al Kα monochromated radiation (1486.7 eV). Spectral fitting was performed using CasaXPS version 2.3.16.

The acid capacities of the synthesized catalysts were determined by acid-base titration while using NaCl solution as an ion-exchange agent. 50 mg sample in powder form was ion-exchanged with 50 mL 2 mol/L NaCl solution at RT for more than 24 h. The filtrates were then titrated with a 0.01 mol/L NaOH solution.

3.4. Catalytic Activity Tests

Catalytic activity were evaluated in the glycerol acetalization with 1,3,5-trioxane (TOX). In a typical experiment, glycerol, TOX, and a certain amount of catalyst were added quantificationally into the reactor. The mixture was heated to a desired temperature and stirred at a speed of 600 rpm/min. Upon reaction completion, the qualitative analysis of products were performed by chromatography/mass spectrometry (GC/MS) (Agilent 7980A/5975C, Santa Clara, CA, USA). The products of the reactions were quantified on an Aglient 7890GC (Santa Clara, CA, USA) using a flame ionization detector (FID) with a HP-5 30 m $\times$ 0.32 mm $\times$ 0.2 μm capillary column.

4. Conclusions

An array of propylsulfonic acid functionalized SBA-15 were prepared while using different methods with different structure parameter and varying amount of propylsulfonic acid group. The propylsufonic acid functionalized KIT-6 catalysts have been prepared by co-condensation under different aging temperature and compared with the series of SBA-15. PrSO$_3$H-SBA-15-400 is the most active catalyst in glycerol acetalization with formaldehyde. The yield of GF and distribution of the GF isomers could be adjusted by varying reaction condition. The glycerol acetalization with TOX was optimized and conducted out under 90 °C, 8 h, with 4 wt % catalyst loading, and the ratio of formaldehyde to glycerol is 1.5:1. PrSO$_3$H-SBA-15-400 showed optimal catalyst activity with 91.5% yield and the ratio of 5R to 6R is 42:58.

Author Contributions: J.C. and R.L. conceived and designed the experiments; R.L. and H.S. performed the experiments and analyzed the data; R.L. and H.S. wrote the paper and proofread the manuscript. All authors discussed the results and commented on the manuscript.

Conflicts of Interest: The authors declare no conflicts of interest.

References

1. Zhou, C.H.; Beltramini, J.N.; Fan, Y.X.; Lu, G.Q. Chemoselective catalytic conversion of glycerol as a biorenewable source to valuable commodity chemicals. *Chem. Soc. Rev.* **2008**, *37*, 527–549. [CrossRef] [PubMed]
2. Sun, D.; Yamada, Y.; Sato, S.; Ueda, W. Glycerol hydrogenolysis into useful C3 chemicals. *Appl. Catal. B Environ.* **2016**, *193*, 75–92. [CrossRef]
3. Katryniok, B.; Paul, S.; Dumeignil, F. Recent Developments in the Field of Catalytic Dehydration of Glycerol to Acrolein. *ACS Catal.* **2013**, *3*, 1819–1834. [CrossRef]
4. Bauer, F.; Hulteberg, C. Is there a future in glycerol as a feedstock in the production of biofuels and biochemicals? *Biofuels Bioprod. Biorefin.* **2013**, *7*, 43–51. [CrossRef]
5. Rühl, C.; Giljum, J. BP Energy Outlook 2030. Presented at International Association for Energy Economics, Stockholm, Sweden, 19–23 June 2011.
6. Wang, Y.; Zhou, J.; Guo, X. Catalytic hydrogenolysis of glycerol to propanediols: A review. *RSC Adv.* **2015**, *5*, 74611–74628. [CrossRef]
7. Kusunoki, Y.; Miyazawa, T.; Kunimori, K.; Tomishige, K. Highly active metal–acid bifunctional catalyst system for hydrogenolysis of glycerol under mild reaction conditions. *Catal. Commun.* **2005**, *6*, 645–649. [CrossRef]
8. Furikado, I.; Miyazawa, T.; Koso, S.; Shimao, A.; Kunimori, K.; Tomishige, K. Catalytic performance of Rh/SiO$_2$ in glycerol reaction under hydrogen. *Green Chem.* **2007**, *9*, 582–588. [CrossRef]
9. Soares, R.R.; Simonetti, D.A.; Dumesic, J.A. Glycerol as a source for fuels and chemicals by low-temperature catalytic processing. *Angew. Chem. Int. Ed.* **2006**, *45*, 3982–3985. [CrossRef] [PubMed]
10. Katryniok, B.; Kimura, H.; Skrzyńska, E.; Girardon, J.S.; Fongarland, P.; Capron, M.; Ducoulombier, R.; Mimura, N.; Paul, S.; Dumeignil, F. Selective catalytic oxidation of glycerol: Perspectives for high value chemicals. *Green Chem.* **2011**, *13*, 1960–1979. [CrossRef]
11. Chai, S.; Wang, H.; Liang, Y.; Xu, B. Sustainable production of acrolein: Gas-phase dehydration of glycerol over Nb$_2$O$_5$ catalyst. *J. Catal.* **2007**, *250*, 342–349. [CrossRef]
12. Pawar, R.R.; Gosai, K.A.; Bhatt, A.S.; Kumaresan, S.; Lee, S.M.; Bajaj, H.C. Clay catalysed rapid valorization of glycerol towards cyclic acetals and ketals. *RSC Adv.* **2015**, *5*, 83985–83996. [CrossRef]
13. Garcia, E.; Laca, M.; Pérez, E.; Garrido, A.; Peinado, J. New Class of Acetal Derived from Glycerin as a Biodiesel Fuel Component. *Energy Fuels* **2008**, *22*, 4274–4280. [CrossRef]
14. Climent, M.J.; Corma, A.; Velty, A. Synthesis of hyacinth, vanilla, and blossom orange fragrances: The benefit of using zeolites and delaminated zeolites as catalysts. *Appl. Catal. A Gen.* **2004**, *263*, 155–161. [CrossRef]
15. Climent, M.J.; Velty, A.; Corma, A. Design of a solid catalyst for the synthesis of a molecule with blossom orange scent. *Green Chem.* **2002**, *4*, 565–569. [CrossRef]
16. Konwar, L.J.; Samikannu, A.; Mäki-Arvela, P.; Boström, D.; Mikkola, J.P. Lignosulfonate-based macro/mesoporous solid protonic acids for acetalization of glycerol to bio-additives. *Appl. Catal. B Environ.* **2018**, *220*, 314–323. [CrossRef]
17. Da Silva, C.X.A.; Gonçalves, V.L.C.; Mota, C.J.A. Water-tolerant zeolite catalyst for the acetalisation of glycerol. *Green Chem.* **2009**, *11*, 38–41. [CrossRef]
18. Trifoi, A.R.; Agachi, P.S.; Pap, T. Glycerol acetals and ketals as possible diesel additives: A review of their synthesis protocols. *Renew. Sustain. Energy. Rev.* **2016**, *62*, 804–814. [CrossRef]
19. Behr, A.; Eilting, J.; Irawadi, K.; Leschinski, J.; Lindner, F. Improved utilisation of renewable resources: New important derivatives of glycerol. *Green Chem.* **2008**, *10*, 13–30. [CrossRef]
20. Showler, A.J.; Darley, P.A. Condensation products of glycerol with aldehydes and ketones 2-substituted m-diloxan-5-ols and 1,3-dioxolane-4-methanols. *Chem. Rev.* **1998**, *67*, 427–440. [CrossRef]
21. Wang, J.; Shen, X.; Chi, R. The Synthesis Method of Glycerol Methyl Acetal. CN Patent 101525329, 9 September 2009.

22. Gras, J.L.; Nouguier, R.; Mchich, M. Transacetalisation de triols a partir du dimethoxymethane. Selectivite et applications synthetiques. *Tetrahedron Lett.* **1987**, *28*, 6601–6604. [CrossRef]

23. Umbarkar, S.B.; Kotbagi, T.V.; Biradar, A.V.; Pasricha, R.; Chanale, J.; Dongare, M.K.; Mamede, A.S.; Lancelot, C.; Payen, E. Acetalization of glycerol using mesoporous MoO_3/SiO_2 solid acid catalyst. *J. Mol. Catal. A Chem.* **2009**, *310*, 150–158. [CrossRef]

24. Dodson, J.R.; Leite, T.; Pontes, N.S.; Peres Pinto, B.; Mota, C.J. Green acetylation of solketal and glycerol formal by heterogeneous acid catalysts to form a biodiesel fuel additive. *ChemSusChem* **2014**, *7*, 2728–2734. [CrossRef] [PubMed]

25. Nair, G.S.; Adrijanto, E.; Alsalme, A.; Kozhevnikov, I.V.; Cooke, D.J.; Brown, D.R.; Shiju, N.R. Glycerol utilization: Solvent-free acetalisation over niobia catalysts. *Catal. Sci. Technol.* **2012**, *2*, 1173–1179. [CrossRef]

26. Reddy, P.S.; Sudarsanam, P.; Mallesham, B.; Raju, G.; Reddy, B.M. Acetalisation of glycerol with acetone over zirconia and promoted zirconia catalysts under mild reaction conditions. *J. Ind. Eng. Chem.* **2011**, *17*, 377–381. [CrossRef]

27. Chen, L.; Nohair, B.; Kaliaguine, S. Glycerol acetalization with formaldehyde using water-tolerant solid acids. *Appl. Catal. A Gen.* **2016**, *509*, 143–152. [CrossRef]

28. Chen, L.; Nohair, B.; Zhao, D.; Kaliaguine, S. Glycerol acetalization with formaldehyde using heteropolyacid salts supported on mesostructured silica. *Appl. Catal. A Gen.* **2018**, *549*, 207–215. [CrossRef]

29. Deutsch, J.; Martin, A.; Lieske, H. Investigations on heterogeneously catalysed condensations of glycerol to cyclic acetals. *J. Catal.* **2007**, *245*, 428–435. [CrossRef]

30. Slowing, I.I.; Vivero-Escoto, J.L.; Trewyn, B.G.; Lin, V.S.Y. Mesoporous silica nanoparticles: Structural design and applications. *J. Mater. Chem.* **2010**, *20*, 7924–7937. [CrossRef]

31. Das, D.; Lee, J.F.; Cheng, S. Selective synthesis of Bisphenol-A over mesoporous MCM silica catalysts functionalized with sulfonic acid groups. *J. Catal.* **2004**, *223*, 152–160. [CrossRef]

32. Dhainaut, J.; Dacquin, J.P.; Lee, A.F.; Wilson, K. Hierarchical macroporous–mesoporous SBA-15 sulfonic acidcatalysts for biodiesel synthesis. *Green Chem.* **2010**, *12*, 296–303. [CrossRef]

33. Mercier, L.; Pinnavaia, T.I. Access in Mesoporous Materials: Advantages of a Uniform Pore Structure in the Design of a Heavy Metal Ion Adsorbent for Environmental Remediation. *Adv. Mater.* **1997**, *9*, 500–503. [CrossRef]

34. Mercier, L.; Pinnavaia, T.J. Heavy Metal Ion Adsorbents Formed by the Grafting of a Thiol Functionality to Mesoporous Silica Molecular Sieves: Factors Affecting Hg(II) Uptake. *Environ. Sci. Technol.* **1998**, *32*, 2749–2754. [CrossRef]

35. Díaz, I.; Márquez-Alvarez, C.; Mohino, F.; Pérez-Pariente, J.N.; Sastre, E. Combined Alkyl and Sulfonic Acid Functionalization of MCM-41-Type Silica. *J. Catal.* **2000**, *193*, 283–294. [CrossRef]

36. Karimi, B.; Mirzaei, H.M.; Mobaraki, A.; Vali, H. Sulfonic acid-functionalized periodic mesoporous organosilicas in esterification and selective acylation reactions. *Catal. Sci. Technol.* **2015**, *5*, 3624–3631. [CrossRef]

37. Jun, S.; Kim, J.M.; Ryoo, R.; Ahn, Y.S.; Han, M.H. Hydrothermal stability of MCM-48 improved by postsynthesis restructuring in salt solution. *Microporous Mesoporous Mater.* **2000**, *41*, 119–127. [CrossRef]

38. Rhijn, W.M.V.; Vos, D.E.D.; Sels, B.F.; Bossaert, W.D.; Jacobs, P.A. Sulfonic acid functionalised ordered mesoporous materials as catalysts for condensation and esterification reactions. *Chem. Commun.* **1998**, 317–318. [CrossRef]

39. Karimi, B.; Mirzaei, H.M.; Mobaraki, A. Periodic mesoporous organosilica functionalized sulfonic acids as highly efficient and recyclable catalysts in biodiesel production. *Catal. Sci. Technol.* **2012**, *2*, 828–834. [CrossRef]

40. Zhang, F.; Yan, Y.; Yang, H.; Meng, Y.; Yu, C.; Tu, B.; Zhao, D. Understanding Effect of Wall Structure on the Hydrothermal Stability of Mesostructured Silica SBA-15. *J. Phys. Chem. B* **2005**, *109*, 8723–8732. [CrossRef] [PubMed]

41. Pirez, C.; Lee, A.F.; Manayil, J.C.; Parlett, C.M.A.; Wilson, K. Hydrothermal saline promoted grafting: A route to sulfonic acid SBA-15 silica with ultra-high acid site loading for biodiesel synthesis. *Green Chem.* **2014**, *16*, 4506–4509. [CrossRef]

42. Dacquin, J.P.; Lee, A.F.; Pirez, C.; Wilson, K. Pore-expanded SBA-15 sulfonic acid silicas for biodiesel synthesis. *Chem. Commun.* **2012**, *48*, 212–214. [CrossRef] [PubMed]

43. Kruk, M.; Jaroniec, M.; Ko, C.H.; Ryoo, R. Characterization of the porous structure of SBA-15. *Chem. Mater.* **2000**, *12*, 1961–1968. [CrossRef]

44. Konwar, L.J.; Das, R.; Thakur, A.J.; Salminen, E.; Mäki-Arvela, P.; Kumar, N.; Mikkola, J.P.; Deka, D. Biodiesel production from acid oils using sulfonated carbon catalyst derived from oil-cake waste. *J. Mol. Catal. A Chem.* **2014**, *388–389*, 167–176. [CrossRef]

45. Konwar, L.J.; Mäki-Arvela, P.; Salminen, E.; Kumar, N.; Thakur, A.J.; Mikkola, J.P.; Deka, D. Towards carbon efficient biorefining: Multifunctional mesoporous solid acids obtained from biodiesel production wastes for biomass conversion. *Appl. Catal. B Environ.* **2015**, *176–177*, 20–35. [CrossRef]

46. Roberts, A.D.; Li, X.; Zhang, H. Hierarchically porous sulfur-containing activated carbon monoliths via ice-templating and one-step pyrolysis. *Carbon* **2015**, *95*, 268–278. [CrossRef]

47. Wang, Z.; Wang, D.; Zhao, Z.; Chen, Y.; Lan, J. A DFT study of the structural units in SBA-15 mesoporous molecular sieve. *Comput. Theor. Chem.* **2011**, *963*, 403–411. [CrossRef]

48. Cano-Serrano, E.; Campos-Martin, J.M.; Fierro, J.L.G. Sulfonic acid-functionalized silica through quantitative oxidation of thiol groups. *Chem. Commun.* **2003**, *0*, 246–247. [CrossRef]

49. da Silva Ferreira, A.C.; Barbe, J.C.; Bertrand, A. Heterocyclic Acetals from Glycerol and Acetaldehyde in Port Wines: Evolution with Aging. *J. Agric. Food Chem.* **2002**, *50*, 2560–2564. [CrossRef] [PubMed]

50. Chopade, S.P.; Sharma, M.M. Acetalization of ethylene glycol with formaldehyde using cation-exchange resins as catalysts: Batch versus reactive distilltion. *React. Funct. Polym.* **1997**, *34*, 37–45. [CrossRef]

51. Agirre, I.; García, I.; Requies, J.; Barrio, V.L.; Guemez, M.B.; Cambra, J.F.; Arias, P.L. Glycerol acetals, kinetic study of the reaction between glycerol and formaldehyde. *Biomass Bioenergy* **2011**, *35*, 3636–3642. [CrossRef]

52. Kleitz, F.; Choi, S.H.; Ryoo, R. Cubic Ia3d large mesoporous silica: Synthesis and replication to platinum nanowires, carbon nanorods and carbon nanotubes. *Chem. Commun.* **2003**, 2136–2137. [CrossRef]

53. Margolese, D.; Melero, J.A.; Christiansen, S.C.; Chmelka, B.F.; Stucky, G.D. Direct Syntheses of Ordered SBA-15 Mesoporous Silica Containing Sulfonic Acid Groups. *Chem. Mater.* **2000**, *12*, 2448–2459. [CrossRef]

54. Burkett, S.L.; Sims, S.D.; Mann, S. Synthesis of hybrid inorganic-organic mesoporous silica by co-condensation of siloxane and organosiloxane precursors. *Chem. Commun.* **1996**, *0*, 1367–1368. [CrossRef]

55. Karimi, B.; Zareyee, D. Design of a Highly Efficient and Water-Tolerant Sulfonic Acid Nanoreactor Based on Tunable Ordered Porous Silica for the von Pechmann Reaction. *Org. Lett.* **2008**, *10*, 3989–3992. [CrossRef] [PubMed]

56. Lim, M.H.; Stein, A. Comparative Studies of Grafting and Direct Syntheses of Inorganic-Organic Hybrid Mesoporous Materials. *Chem. Mater.* **1999**, *11*, 3285–3295. [CrossRef]